

Antisense inhibition of Bcr-Abl/c-Abl synthesis promotes telomerase activity and upregulates tankyrase in human leukemia cells¹

Rumiana Bakalova^{a,*}, Hideki Ohba^a, Zhivko Zhelev^a, Takanori Kubo^b, Masayuki Fujii^{b,c}, Mitsuru Ishikawa^a, Yasuo Shinohara^{a,d}, Yoshinobu Baba^{a,d}

^aSingle-Molecule Bioanalysis Laboratory, National Institute for Advanced Industrial Science and Technology, AIST-Shikoku, 2217-14 Hayashi-cho, Takamatsu, Kagawa 761-0395, Japan

^bDepartment of Chemistry, Kyushu School of Engineering, Kinki University, 11-6 Kayanomori, Iizuka, Fukuoka 820-8555, Japan

^cMolecular Engineering Institute, Kinki University, 11-6 Kayanomori, Iizuka, Fukuoka 820-8555, Japan

^dFaculty of Pharmaceutical Science, Tokushima University, Tokushima, Japan

Received 28 January 2004; revised 3 March 2004; accepted 14 March 2004

First published online 26 March 2004

Edited by Varda Rotter

Abstract Clinical studies in chronic myelogenous leukemia demonstrate that the overexpression of Bcr-Abl tyrosine kinase is usually accompanied by relatively low telomerase activity in the chronic phase, which reverts to a high activity in blast crisis. The present study was designed to investigate the cross-talk between both enzymes, using Bcr-Abl-positive K-562 and Bcr-Abl-negative Jurkat cell lines, treated with antisense oligodeoxynucleotides (ODNs) against Bcr-Abl/c-Abl mRNA. The decreased amount and enzyme activity of Bcr-Abl/c-Abl provoked telomerase activation in both cell lines. After short-term treatment with anti-Bcr-Abl/c-Abl ODNs (6 days), no variations in hTERT and phospho-hTERT were detected. The decreased amount of Bcr-Abl/c-Abl was accompanied by: alterations in telomeric associated proteins—overexpression of tankyrase and decreased amount of TRF1/Tin2, cell growth arrest of K-562 cells, reaching a plateau after 6 days treatment, and increased proliferating activity of Jurkat cells. No changes in telomere length were detected after short-term treatment. In contrast, after long-term treatment with anti-Bcr-Abl/c-Abl ODNs (36 days), a significant elongation of telomeres and enhancement of hTERT were established, accompanied by an increased proliferating activity of both cell lines. These data provide evidence that the inhibition of Bcr-Abl or c-Abl synthesis keeps a potential to restore or induce cell proliferation through telomere lengthening control and telomerase activation.

© 2004 Federation of European Biochemical Societies. Published by Elsevier B.V. All rights reserved.

Key words: Bcr-abl tyrosine kinase; Telomerase; Telomeric associated proteins; Cross-talk; Chronic myelogenous leukemia

1. Introduction

The Bcr-Abl oncogene is a result of a reciprocal translocation between the long arms of chromosomes 9 and 22 (known as Philadelphia (Ph) chromosome; t(9;22)), encoding a cytoplasmic protein with constitutive tyrosine kinase activity that inhibits apoptosis. There is good experimental evidence demonstrating that Bcr-Abl is a single causative abnormality in chronic myelogenous leukemia (CML), at least in the chronic phase, making it a unique model for the development of molecular targets for disease control [1–3]. The increased knowledge of Bcr-Abl has resulted in the design of several novel therapeutic approaches, including highly specific tyrosine kinase inhibitors (such as Glivec and pyrido[2,3-*d*]pyrimidine derivative PD180970), antisense strategies and immunomodulation [1–4].

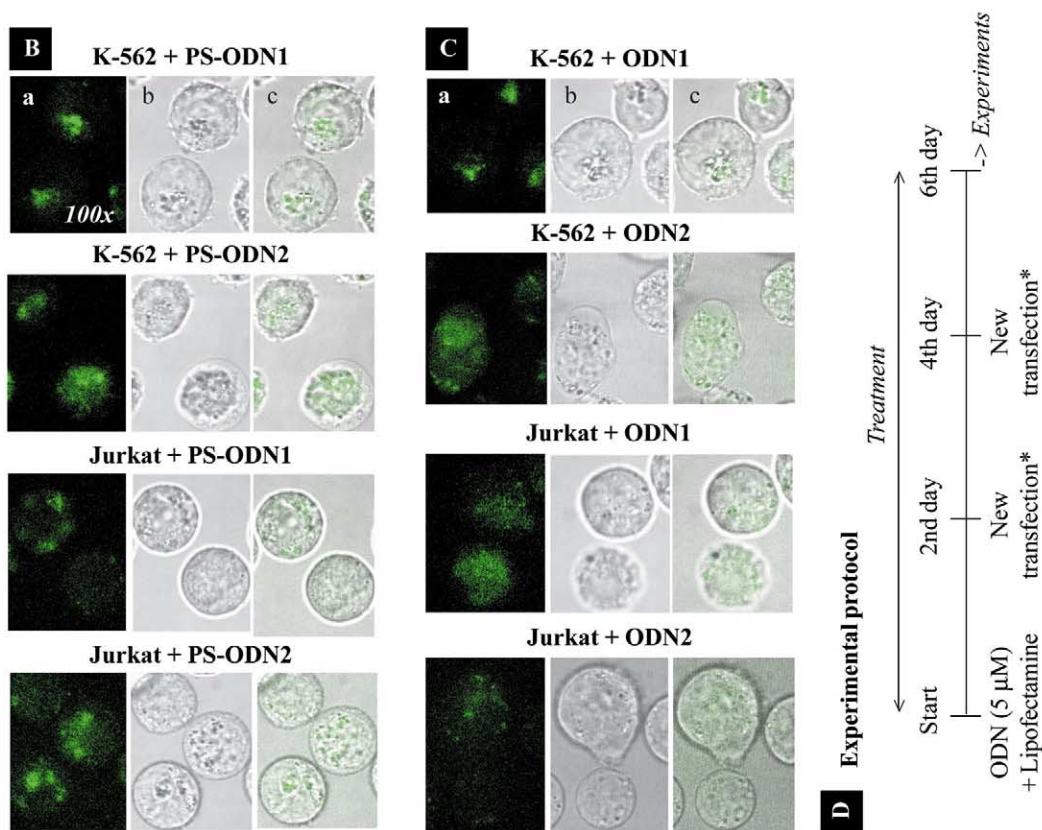
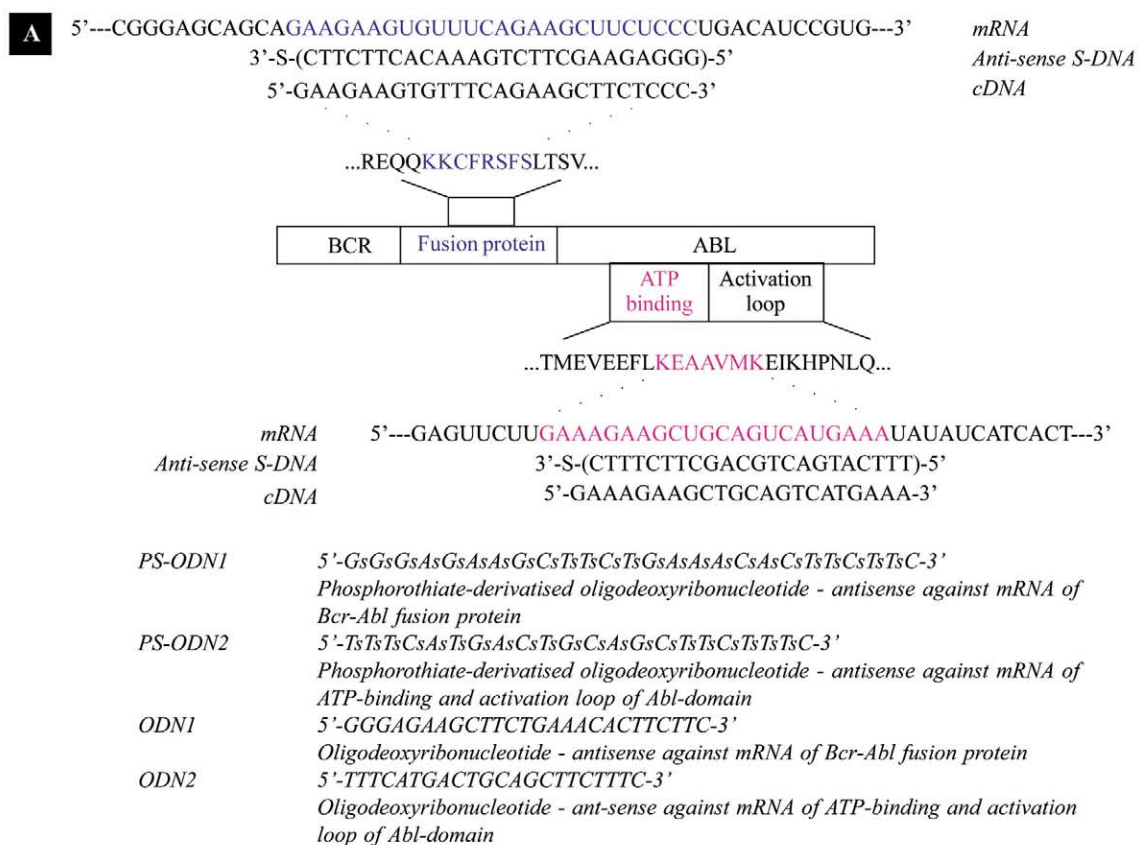
The chronic phase of CML is also unique, in comparison with other types of leukemia, with its relatively low telomerase activity [5]. Approximately 80% of CML patients in the chronic phase show reduced telomere length and low telomerase activity, in contrast to a large number of tumors and immortalized cell lines in which telomerase is overexpressed [5–7]. However, during CML progression to the acute phase, termed blast crisis, more than 60% (up to 80%) of patients show additional cytogenetic changes, resulting in genome instability, enhanced telomerase activity and telomere dynamics [5,7]. It has been observed that the telomerase activity has a high prognostic impact for CML and its enhancement is associated with shorter survival of the patients. It seems that both abnormalities responsible for immortalization of Ph(+) leukemia cells – Bcr-Abl tyrosine kinase and telomerase – are essential in equal degrees for the exit of the disease. With the advent of new anti-CML drugs, it is important to clarify whether cross-talk exists between both key enzymes, how the drugs influence this relationship, how this plays a functional role in CML progression and at relapse with the development of chemotherapy resistance.

The catalytic core of human telomerase consists of an RNA template, a catalytic protein subunit with reverse transcriptase activity (hTERT) and additional telomerase-associated proteins [8,9]. hTERT is considered a phosphoprotein. Its reversible phosphorylation by a complex set of protein kinases seems to be a prerequisite for modulation of telomerase activity and its connection with signal transduction pathways [10–12]. Two antagonistic protein kinase-dependent mecha-

*Corresponding author.

E-mail address: r.bakalova-zheleva@aist.go.jp (R. Bakalova).

¹ The GenBank accession numbers for human Bcr-Abl and human c-Abl cDNA sequences described in this paper are X02596/M24603 and X16416, respectively. ODN1/PS-ODN1 antisense sequences and ODN3/PS-ODN3 control sense sequences correspond to the nucleotide sites localized in the breakpoint cluster region (b3a2 junction) in the 9:22 chromosomal translocation (Philadelphia chromosome, accession numbers X02596 and M24603, version X02596.1, between ex. 3061 and 3121). ODN2/PS-ODN2 antisense sequences and ODN4/PS-ODN4 control sense sequences correspond to the nucleotide site of Abl proto-oncogene, localized between ex. 961 and 1021 (accession number X16416, version X16416.1). ODN5 and PS-ODN5 are nonsense sequences and did not show homology with both cDNAs.



nisms for telomerase regulation have been described: (1) protein kinase C/B-dependent activation [10,11], and (2) c-Abl-dependent inhibition of the enzyme [12].

Proceeding from the fact that Bcr-Abl fusion strongly activates Abl tyrosine kinase and therefore potentiates telomerase suppression in Ph(+) cells, it is possible to explain, at least partially, the relatively low telomerase activity in the chronic phase of CML. It has been established that other chromosomal translocations that generate fusion proteins (for example Tel-Abl) are also characterized by enhanced Abl-tyrosine kinase activity and low telomerase activity [7]. A 'vicious circle' seems to take place in Ph(+) cells and selective c-Abl inhibitors would have a potential to restore cell immortalization through telomerase activation.

On the other hand, recently it has been reported that protein kinase (PK) C α activity is necessary for Bcr-Abl-mediated resistance to drug-induced apoptosis [13]. Inhibition of Bcr-Abl using the highly selective inhibitor tyrphostin AG957 completely abolishes PKC α activation and sensitizes (Ph+) K-562 cells to drug-induced apoptosis. Therefore, the selective Bcr-Abl inhibitors also possess a potential to suppress telomerase indirectly through the inhibition of atypical PKC isoenzymes.

Obviously, there is a fine link between Bcr-Abl tyrosine kinase and telomerase in CML and the efficacy of drug therapy depends on this relationship. During disease progression chemotherapy can restore or avoid the immortalization of Ph(+) cells through direct or indirect (PK-mediated) telomerase control, regardless of its strong and selective inhibitory effect on Bcr-Abl. A good understanding of the cross-talk between telomerase and Bcr-Abl tyrosine kinase is potentially useful for development of a new strategy for CML control and for decrease of resistance to the drug-target therapy.

The present study was designed to investigate this relationship, using (Ph+) K-562 cells, treated with antisense oligodeoxynucleotides (ODNs) against mRNA for fusion protein and the ATP-binding loop of the Bcr-Abl molecule. As a negative control Ph-negative (Ph-) Jurkat cells were tested.

2. Materials and methods

2.1. ODNs

The sense mRNA/cDNA sites and antisense sequences are shown in Fig. 1A. Two types of ODNs were used: phosphorothioate-derivatized (PS-ODN1 and PS-ODN2) and non-derivatized (ODN1 and ODN2, termed 'native'). The following non-derivatized and PS-derivatized sense and nonsense sequences were used as negative controls: ODN3 (Bcr-Abl sense), 3'-S-CCCTCTTCGAAGACTTTGTGAAG-5'; ODN4 (c-Abl sense), 3'-S-AAAGTACTGACGTCGAAGAAAG-5'; ODN5 (nonsense), 3'-S-AAGTTTGTCTTAAAGGACAG-5'.

2.2. Cells and transfection protocol

K-562 (derived from CML patients in blast crisis) and Jurkat cells (derived from patients with acute lymphoblastic leukemia, ALL) were a generous gift of Dr. J. Minowada (Hayashibara Biochemical Laboratories, Okayama, Japan). The cells were cultured in RPMI 1640 medium, supplemented with 10% heat-inactivated fetal bovine serum in a humidified atmosphere at 37°C with 5% CO $_2$. The cells used for transfection were about 80% confluent.

Transfection conditions: collection of cells by centrifugation, resuspension of cells in a new medium to 8×10^5 cells/ml, ODN (5 μ M) transfection using lipofectamine (6 h), replacement of cells in a new medium (4×10^5 cells/ml) and cultivation in a humidified atmosphere. The conditions for preparation of ODN-lipofectamine complexes are described in the Lipofectamine 2000 protocol (Invitrogen).

2.3. Fluorescent confocal microscopy – ODN delivery into the cells

Cells (2×10^5 /ml) were cultured for 24 h in the presence of fluorescein isothiocyanate (FITC)-labeled PS-ODN1 or FITC-PS-ODN2 (single dose 1 μ M), or transfected with FITC-labeled ODNs (single dose 1 μ M) using lipofectamine as described above. Six hours transient transfection was applied and transfected cells were cultured in RPMI 1640 medium. At 24 h post transfection (in the case of ODNs) or 24 h incubation (in the case of PS-ODNs) the cells were sedimented by centrifugation ($1000 \times g/10$ min), washed twice with phosphate-buffered saline (PBS) (Ca $^{2+}$ - and Mg $^{2+}$ -free) to eliminate free fluorescent PS-ODN molecules outside the cells, and the FITC-labeled PS-ODNs, incorporated into living cells (green spots), were detected by fluorescent confocal microscopy. The samples were analyzed with an Olympus IX70 microscope.

2.4. Telomerase activity assay

Telomerase activity was detected by a conventional telomeric repeat amplification protocol (TRAP) and the Stretch polymerase chain reaction (PCR) method, using the Telomerase assay kit (TeloChaser, Toyobo), with slight modifications. Briefly, the cells (2×10^4) were lysed in 25 μ l TeloChaser buffer (containing protease and phosphatase inhibitor cocktail, Toyobo) for 30 min, at 4°C. The sample was centrifuged at $12000 \times g/20$ min, at 4°C. The supernatant was used in the next procedure. Telomerase activity was assayed by a two-step process: (i) telomerase-mediated extension (20 min, 30°C) of an oligonucleotide (TAG-U primer, containing telomeric repeats), and (ii) PCR amplification of the resulting product using forward and reverse primers [14]. The PCR reaction consisted of 32 cycles (30 s at 95°C, 30 s at 68°C, and 45 s at 72°C). GeneAmp PCR System 9700 (Applied Biosystems) was used. The product of telomerase reaction was analyzed by TBA electrophoresis in a non-denaturing 12% polyacrylamide gel. Gels were stained with Silver Staining kit (Pharmacia Biotech), according to the manufacturer's instruction. As a negative control, an aliquot of each sample was incubated at 70°C for 10 min to inactivate telomerase.

2.5. Immunoblot analyses

2.5.1. Bcr-Abl/c-Abl detection. The cells were treated with antisense ODNs as shown in Fig. 1D. Aliquots of 4×10^5 cells were lysed in TeloChaser buffer (containing protease and phosphatase inhibitor cocktail) for 30 min at 4°C, centrifuged at $12000 \times g/20$ min/4°C and supernatant was dissolved 1:1 in 2 \times Laemmli sample buffer (1.1 M Tris-HCl, pH 6.0, 3.3% sodium dodecyl sulfate (SDS), 22% glycerol, 10% β -mercaptoethanol, 0.001% bromophenol blue). Samples (with

Fig. 1. A: Sequences of chemically synthesized antisense ODNs against Bcr-Abl/c-Abl mRNA. B: Penetration of phosphorothioate (PS)-derivatized ODNs (green spots) into living Ph(+) K-562 and Ph(-) Jurkat cells. Cells (2×10^5 /ml) were cultured for 24 h in the presence of FITC-labeled PS-ODNs as described in Section 2. The cells were sedimented by centrifugation, washed twice with PBS (Ca $^{2+}$ - and Mg $^{2+}$ -free), and FITC-labeled antisense substances, incorporated into living cells (green spots), were detected by fluorescent confocal microscopy. Quadrant a: fluorescence; quadrant b: transmission; quadrant c: fluorescence and transmission. In the case of native ODNs (ODN1 and ODN2), no fluorescence was detected in living K-562 and Jurkat cells (data not shown). C: Penetration of ODNs into living Ph(+) K-562 and Ph(-) Jurkat cells after transient transfection with lipofectamine. Cells (2×10^5 /ml) were transfected during 6 h with FITC-labeled ODNs using lipofectamine and the procedure described in Section 2. At 24 h post transfection, the cells were sedimented by centrifugation, washed twice with PBS (Ca $^{2+}$ - and Mg $^{2+}$ -free), and FITC-labeled antisense substances, incorporated into living cells (green spots), were detected by fluorescent confocal microscopy. Quadrant a: fluorescence; quadrant b: transmission; quadrant c: fluorescence and transmission. In the case of PS-ODNs, the data were analogous to these in B. D: Scheme of 'chronic' treatment of K-562 and Jurkat cells by antisense ODNs. *New transfection conditions: collection of cells by centrifugation, resuspension of cells in a new medium to 2×10^5 cells/ml, ODN (5 μ M) transfection using lipofectamine (6 h), replacement of cells in a new medium and cultivation in a humidified atmosphere.

equal protein concentrations) were heated at 95°C for 10 min and were applied to 5% stacking, 4–12% resolving SDS–polyacrylamide gel. Electrophoresis was carried out in two steps: at 80 V for 15 min, 120 V for 2 h at room temperature (RT, ~22°C). Bio-Rad Kaleidoskop protein standards were also applied for comparison. After electrophoresis the separated protein fractions were transferred to a Hybond-P polyvinylidene difluoride (PVDF) membrane (Amersham Bioscience) using the XCell II Blot Module (Novex). The transfer was carried out at 35 V for 18 h at 4°C. The membranes were cut at 45 kDa (for β -actin) and 150–210 kDa (for c-Abl and Bcr-Abl) molecular weight levels. A double antibody procedure was used to detect the proteins. The membranes were incubated under agitation for 1 h at RT in a blocking solution (PBS, containing 5% dry skimmed milk and 0.1% Tween-20), then at RT for 1 h in anti-c-Abl (rabbit, Sigma; 1:100 dilution for Bcr-Abl and 1:500 for c-Abl detection) or anti- β -actin monoclonal antibodies (mouse, Calbiochem; 1:20000). The antibody solution was removed and the membranes were washed three times with PBS containing 0.1% Tween-20. The membranes were then incubated (1 h at RT under agitation) with horseradish peroxidase (HRP)-conjugated goat anti-rabbit IgG (Sigma, 1:5000) – for anti-c-Abl, and goat anti-mouse IgM (Sigma, 1:2000) – for anti- β -actin antibody. Chemiluminescence was detected immediately using the ECL Advance Western Blotting Detection kit (Amersham Bioscience).

2.5.2. hTERT (127 kDa) detection. The cells were lysed in TeloChaser buffer and applied to SDS electrophoresis and immunoblotting procedures, as described above. Anti-hTERT (rabbit, Calbiochem, 1:1000 diluted) was used as a primary antibody.

An immunoprecipitation procedure was applied before immunoblotting to register phospho-Tyr-hTERT (P-hTERT). hTERT was immunoprecipitated from cell lysates using 0.4 μ g/ml anti-hTERT antibody (rabbit, Calbiochem), according to the method of Li et al. [15]. Antigen–antibody complexes were collected on protein G beads, washed twice with TeloChaser buffer, and suspended 1:1 in 2 \times Laemmli buffer. Samples were fractionated by 5% stacking, 8% resolving SDS–polyacrylamide gel. Proteins were transferred to a Hybond-P PVDF membrane and immunoblotted (no dry skimmed milk

was used in a blocking procedure), using anti-hTERT antibody (rabbit, Calbiochem, 1:1000) as a primary antibody, and anti-rabbit HRP-conjugated anti-phospho-Tyr antibody as a secondary one (Chemicon, 1:1500).

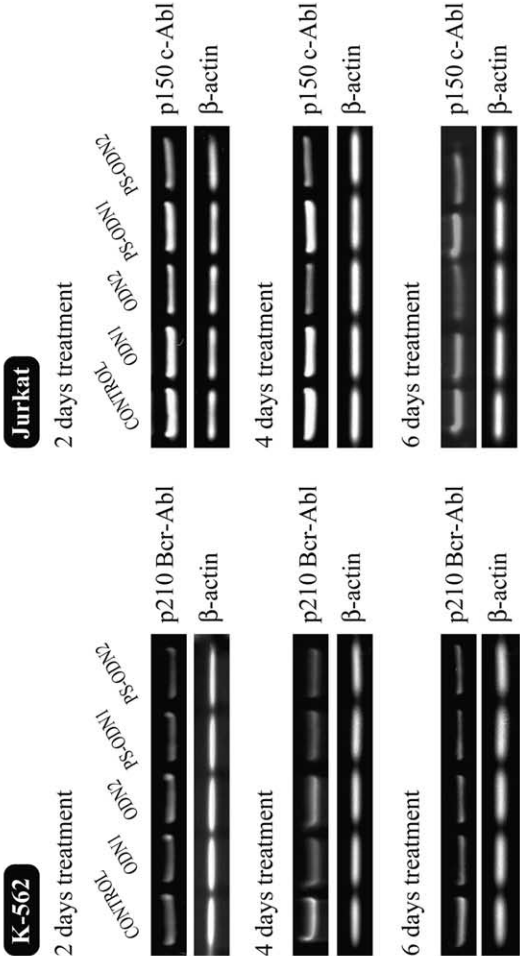
2.5.3. TRF1 (~56 kDa), Tin2 (~40 kDa) and tankyrase (~142 kDa) detection. The cells were lysed in TNE buffer (10 mM Tris, pH 7.8, 1% Nonidet P-40, 0.15 M NaCl, 1 mM EDTA, protease inhibitor cocktail from Sigma) for 1 h at 4°C. After centrifugation at 14000 \times g for 10 min, the supernatant was treated with rabbit IgG and protein G-Sepharose on ice for 20 min. Non-specific antibody complexes and protein aggregates were removed by centrifugation, and the supernatant was used for immunoblot analysis. Endogenous β -actin was used as an internal standard. The supernatant was added to 2 \times Laemmli buffer (1:1, v:v). Samples were fractionated by 5% stacking, 4–20% resolving SDS–polyacrylamide gel. Proteins were transferred to a Hybond-P PVDF membrane and immunoblotted. The following primary antibodies were used: anti-tankyrase (rabbit, Calbiochem, 0.1 μ g/ml), anti-TRF1 (rabbit, Calbiochem, 0.7 μ g/ml), anti-Tin2 (mouse, Calbiochem, 0.5 μ g/ml), anti- β -actin (mouse, Sigma). The respective secondary antibodies (goat anti-rabbit or anti-mouse IgG), conjugated with HRP, were applied. Chemiluminescence of the blots was detected immediately using ECL Advance Western Blotting Detection kit.

2.6. Flow cytometry

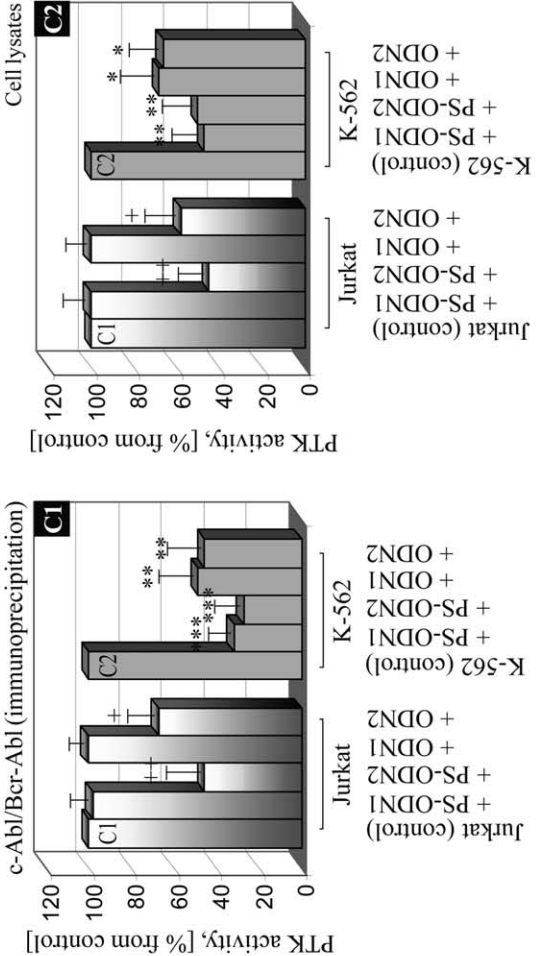
Anti-c-Abl antibody (rabbit, Sigma) was labeled by ZenonAlexa Fluor-488 Rabbit IgG Labeling kit (Molecular Probes). Permeabilization of cells for Fluor-488-conjugated anti-c-Abl antibody was carried out with IntraPrep Permeabilization Reagent (Immunotech). The antibody–antigen interaction was detected by flow cytometry (Beckman Coulter-Epics XL). Data were collected and analyzed with XL System II software. No cells were excluded from the analysis and ~5000 cells were counted. Data are presented as a dot plot of Fluor-488 fluorescence (side scatter, y-axis in 0–128 scale, vs. Fluor-488-conjugated antibody, x-axis in –1–1000 scale) with quadrant markers drawn to distinguish the cells containing different levels of antibody–antigen complexes.

Fig. 2. A: Effect of anti-Bcr-Abl/c-Abl ODNs on the levels of Bcr-Abl (210 kDa) and c-Abl (150 kDa) proteins in Ph(+) K-562 and Ph(–) Jurkat cells, respectively – Western blot analysis. The cells were treated with antisense ODNs as shown in Fig. 1D. Cell lysates were obtained after 2, 4 and 6 days treatment as described in Section 2. The samples (at equal protein concentrations) were dissolved 1:1 in 2 \times Laemmli buffer, heated at 95°C for 10 min and subjected to SDS–polyacrylamide gel electrophoresis (80 V, 15 min; 120 V, 2 h at RT). The separated protein fractions were transferred to a Hybond-P PVDF membrane overnight at 35 V (4°C). The membranes were cut at 45 kDa (for β -actin) and 150–210 kDa (for c-Abl/Bcr-Abl) and were incubated as follows: 1 h at RT in a blocking solution, 1 h in anti-c-Abl antibody (rabbit, Sigma, 1:100 for detection of Bcr-Abl and 1:500 for detection of c-Abl) or in anti- β -actin antibody (mouse, Calbiochem, 1:20000), 1 h with HRP-conjugated goat anti-rabbit IgG (Sigma, 1:5000) for anti-c-Abl or goat anti-mouse IgM (Sigma, 1:2000) for anti- β -actin. Chemiluminescence was detected immediately using ECL Advance Western Blotting Detection kit. Blots from one typical experiment for each protein are shown in the figure. Control blots are representative for non-treated cells, cells treated with lipofectamine only, and for cells transfected with sense or non-sense ODNs/PS-ODNs. B: Effect of anti-Bcr-Abl/c-Abl ODNs (6 days treatment) on the level of Bcr-Abl and c-Abl proteins in Ph(+) K-562 and Ph(–) Jurkat cells, respectively – flow cytometric analysis. The cells were treated with antisense ODNs during 6 days as shown in Fig. 1D. Anti-c-Abl (rabbit, Sigma) was labeled by ZenonAlexa Fluor-488 Rabbit IgG Labeling kit. Permeabilization of cells for Fluor-488-conjugated anti-c-Abl was carried out by IntraPrep permeabilization reagent (Immunotech). The antibody–antigen interaction was detected by flow cytometry as described in Section 2. Data are presented as a dot plot of Fluor-488 fluorescence (side scatter, SS – y-axis in 0–128 scale, vs. Fluor-488-conjugated antibody, Fluor-488 – x-axis in –1–1000 scale) with quadrant markers drawn to distinguish the cells containing different levels of antibody–antigen complexes. In the histograms, quadrant H corresponds to the cells containing the maximum level of c-Abl/Bcr-Abl (positive control), quadrant G corresponds to the cells without fluorescent marker and therefore without c-Abl/Bcr-Abl–antibody complexes (spontaneous cell fluorescence, negative control), and quadrant E (between H and G) corresponds to the cells containing a moderate or low level of Fluor-488-conjugated c-Abl antibody and therefore expressing moderate or lower levels of c-Abl/Bcr-Abl protein in comparison with the positive control. To the right of each histogram Fluor-488 fluorescent curves are drawn. Histograms from one typical experiment are shown in the figure. Positive controls are representative for cells treated with lipofectamine only, and for cells transfected with sense or nonsense ODNs/PS-ODNs. C: Effects of anti-Bcr-Abl/c-Abl ODNs (6 days treatment) on the tyrosine kinase activity in Ph(+) K-562 and Ph(–) Jurkat cells. The cells were treated with antisense ODNs during 6 days as shown in Fig. 1D. Bcr-Abl and/or c-Abl were isolated from cell lysates by immunoprecipitation, using anti-c-Abl antibody (Sigma, 3 μ g/ml) and protein A/G agarose beads. The tyrosine kinase activity of immunoprecipitated enzymes (C1) as well as of cell lysates (C2) was analyzed spectrophotometrically, using Chemicon's PTK Assay kit. The fraction of phosphorylated substrate was visualized at 450 nm, using HRP-conjugated anti-phosphotyrosine antibody (clone PY20) and ensuing chromogenic substrate reaction. The data are presented as means \pm S.D. from eight independent experiments. They were calculated as a percentage of control tyrosine kinase activity, analyzed in non-treated cells. The values of PTK activity in control groups (C1, C2) were considered as 100%. In non-treated cells, the absolute values of P-Tyr-peptide substrate (accumulated for 60 min at 37°C in the presence of immunoprecipitated PTK) were 12.60 \pm 1.25 and 17.48 \pm 1.67 ng for Jurkat and K-562 respectively. In the case of cell lysates, the absolute values of P-Tyr-peptide substrate obtained from non-treated Jurkat or K-562 cells were 11.22 \pm 1.15 and 14.65 \pm 1.07 ng, respectively. OD_{450nm} = 1.0 corresponds to 20 ng P-Tyr-peptide substrate. The calibration curve was linear in the range 10–40 ng P-Tyr-peptide substrate. Control groups are representative for non-treated cells, cells treated with lipofectamine only, and for cells transfected with sense or nonsense ODNs/PS-ODNs. +*P* < 0.05 vs. C1, ++*P* < 0.01 vs. C1, +++*P* < 0.001 vs. C1; **P* < 0.05 vs. C2, ***P* < 0.01 vs. C2, ****P* < 0.001 vs. C2.

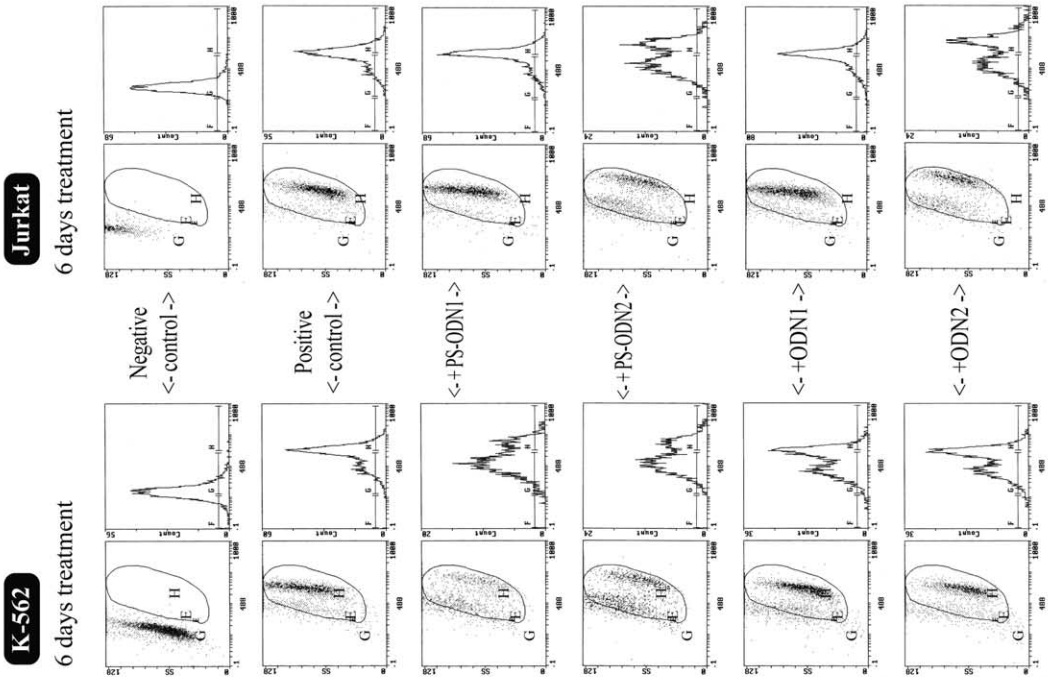
A. Western blot analysis



C. Tyrosine kinase activity assay (6 days treatment)



B. Flow cytometric analysis



2.7. Tyrosine kinase activity test

The cells were sedimented by centrifugation ($1000\times g/10$ min), washed twice with PBS (Ca^{2+} - and Mg^{2+} -free) and resuspended in lysis buffer (TeloChaser). Lysis was carried out for 30 min at 4°C . The cytosolic fraction, containing Bcr-Abl and/or c-Abl, was obtained after centrifugation at $12000\times g/10$ min, 4°C . Bcr-Abl and/or c-Abl proteins were isolated by immunoprecipitation, using anti-c-Abl antibody (Sigma, 3 $\mu\text{g}/\text{ml}$) and protein A/G agarose beads. The tyrosine kinase activity of immunoprecipitated enzyme as well as of cell lysates was analyzed spectrophotometrically, using Chemicon's protein tyrosine kinase (PTK) assay kit. Briefly, a synthetic biotinylated poly-[Glu:Tyr], 4:1 (2.5 $\mu\text{g}/\text{ml}$), containing multiple tyrosine residues, was used as a PTK substrate. The PTK reaction was started by 1 mM ATP/10 mM MgCl_2 and continued for 60 min at 37°C . The enzyme reaction was stopped by addition of 100 mM EDTA and both phosphorylated and dephosphorylated substrates were immobilized on streptavidin-coated plate. The fraction of phosphorylated substrate was visualized spectrophotometrically at 450 nm, using HRP-conjugated mouse anti-phosphotyrosine antibody (clone PY20) and an ensuing chromogenic substrate reaction. The quantity of phosphate incorporated into the tyrosine kinase substrate was determined utilizing the phosphopeptide standard curve.

2.8. Apoptosis detection

2.8.1. Annexin V-FITC test (Beckman Coulter). The exposure of phosphatidylserine (PSer) on the cell surface was used as a criterion for early apoptotic events. Cells ($2\times 10^5/\text{ml}$) were cultured as described in Fig. 1D. After collection by centrifugation they were washed twice with PBS, containing 2.5 mM CaCl_2 (annexin V binding buffer). 100 μl of the cell suspension was incubated with 5 μl of FITC-conjugated annexin V (FITC-annexin V) for 10 min at RT in the dark. The cells were washed twice with annexin binding buffer and resuspended in 100 μl of the same buffer. FITC-annexin V, bound to PSer on the cell surface, was detected spectrofluorometrically at $\lambda_{\text{em}} = 535$ nm ($\lambda_{\text{ex}} = 488$ nm), using a Fluoromark fluorescent microplate reader (Bio-Rad).

2.8.2. DNA ladder detection test (Waco). DNA fragmentation was used as a criterion for the last phase of apoptosis. The test is based on the fact that DNA from apoptotic cells forms a ladder on the gel, while DNA from non-apoptotic cells appears as a single band or smeared on the gel. Cells ($2\times 10^5/\text{ml}$) were cultured as described in Fig. 1D. The lysis of cells and DNA isolation was carried out according to the test's protocol. DNA was analyzed by TBA electrophoresis in a non-denaturing 6% polyacrylamide gel. Gels were stained with SYBR Green (Sigma), according to the manufacturer's instructions.

2.9. Cell growth arrest

Cells ($2\times 10^5/\text{ml}$) were cultured (in the presence or in the absence of ODNs) as described in Fig. 1D. At each time point cell growth was detected spectrophotometrically, using the CellTiter AQ Proliferation Assay kit (Promega). The method is based on the detection of the number of viable cells in proliferation. In the presence of an electron coupling reagent (phenazine methosulfate) a tetrazolium compound (MTS) is reduced from cells into a formazan product, based on the method of Mosmann [16]. The absorbance of formazan product at 490 nm ($\text{OD}_{490\text{nm}}$) is recorded using 96-well plate reader InterMedImmunomini NJ-2300 (InterMed, Japan).

2.10. Flow-FISH analysis of telomere length

Telomere length was detected by flow cytometry using fluorescence in situ hybridization (FISH) with FITC-labeled peptide nucleic acid (PNA) probes. Details of the protocol are described in Baerlocher et al. [17]. In brief, the cell pellet (5×10^6 for each sample) was resuspended and incubated for 10 min at RT in 200 μl hybridization mixture, containing 75% deionized formamide, 20 mM Tris, pH 7.1, 1% (w/v) bovine serum albumin (BSA) and 20 mM NaCl with either no probe (unstained control) or 0.35 $\mu\text{g}/\text{ml}$ telomere specific FITC-conjugated (C_3TA_3)₃ PNA probe for stained samples (Applied Biosystems). DNA denaturation was carried out in a circulating water bath for 15 min at 87°C . The telomere PNA probe was hybridized for 90 min at RT in the dark. To remove excess and non-specifically bound telomere PNA probe, four washes were performed at RT with 1 ml washing solution (75% formamide, 10 mM Tris, 0.1% BSA, 0.1% Tween-20) followed by centrifugation at $1500\times g$ for 5 min at 16°C . The last wash step was performed with 1 ml washing solution, con-

taining 5% glucose, 10 mM HEPES, 0.1% BSA and 0.1% Tween-20, and centrifugation at $900\times g$ for 5 min at 16°C . After the last wash, the cells were resuspended in a FACSFlow solution (Becton Dickinson), containing 0.1% (w/v) BSA, RNase A (10 $\mu\text{g}/\text{ml}$, Boehringer) and LDS-751 (0.01 $\mu\text{g}/\text{ml}$, Exciton Chemicals) for at least 20 min before acquisition on the flow cytometer. The light scatter and fluorescence signals were performed on a FACSCalibur (Becton Dickinson). A mixture of four populations of FITC-labeled beads (Flow Cytometry Standards) was run for each experiment to convert fluorescence into molecular equivalents of soluble fluorochrome (MESF). Cells hybridized without the FITC-labeled telomere PNA probe were used to correct their autofluorescence. The telomere fluorescence was calculated by subtraction of the autofluorescence of unstained controls from the telomere fluorescence in cells hybridized with FITC-labeled telomere PNA probe. The mean of duplicates was calculated for each sample. The results are expressed as telomere fluorescence in MESF and are means \pm S.E.M. from five independent experiments. The specific fluorescence of control cells (cow thymocytes) served as an internal standard. It was used to convert the MESF values of cells of interest into an average telomere length (in kb) by the formula described from Baerlocher and Lansdorp [18].

2.11. Statistical analysis

One-way analysis of variance was employed, followed by Bonferroni's test for truly significant differences. Statistical significance was defined as $P < 0.05$. The statistical procedures were performed with GraphPad InStat software, version 2.04, USA. Data are expressed as mean \pm S.D.

3. Results and discussion

The structures of chemically synthesized antisense substances are shown in Fig. 1A. They were phosphorothioate-derivatized (PS-ODN1 and PS-ODN2) and non-derivatized (ODN1 and ODN2). Two mRNA sense sequences were chosen. The first target for antisense ODNs was localized in the Bcr-Abl mRNA major breakpoint, which is characterized by a Bcr exon 3/Abl exon 2 (b3a2) junction – a unique sequence in Ph(+) CML cells. The second target was localized in Bcr-Abl mRNA, encoding the ATP binding and activation loop of the following proteins – p210 Bcr-Abl and p150 c-Abl. The selection aimed to avoid the area most sensitive for point mutations in the Abl part around Tyr³¹⁵, responsible for Bcr-Abl amplification and development of drug resistance (as has been described in the clinical trials with Glivec [19–21]). In this case, the structure of antisense ODNs can guarantee the interaction with Bcr-Abl and c-Abl mRNA, despite possible point mutations during the 'chronic' treatment. The structure of PS-ODN2/ODN2 also guarantees the interaction with c-Abl mRNA in Ph(–) Jurkat cells.

The intracellular uptake of the antisense substances was detected by fluorescent confocal microscopy, using FITC as a fluorescent marker (Fig. 1B,C). FITC-labeled PS-ODN1 and PS-ODN2 were detected in the cells after 24 h incubation at 37°C , without any transfection with lipofectamine (Fig. 1B, green spots). Both substances were localized in the cells (in high density sites of K-562 and very sporadically located in Jurkat). In contrast, FITC-labeled ODN1 and ODN2 were unable to enter K-562 and Jurkat cells up to 72 h incubation (no fluorescent conjugates were detected in the cells, data not shown). This is in agreement with already published observations demonstrating that free ODNs do not penetrate or hardly penetrate cell membranes in the absence of a specific carrier [22–24]. However, after transfection using lipofectamine, both antisense substances were detected in the cells after 24 h incubation. Analogous to PS-ODN1/PS-ODN2, the localization of ODN1/ODN2 was most sporadic in Jurkat, and

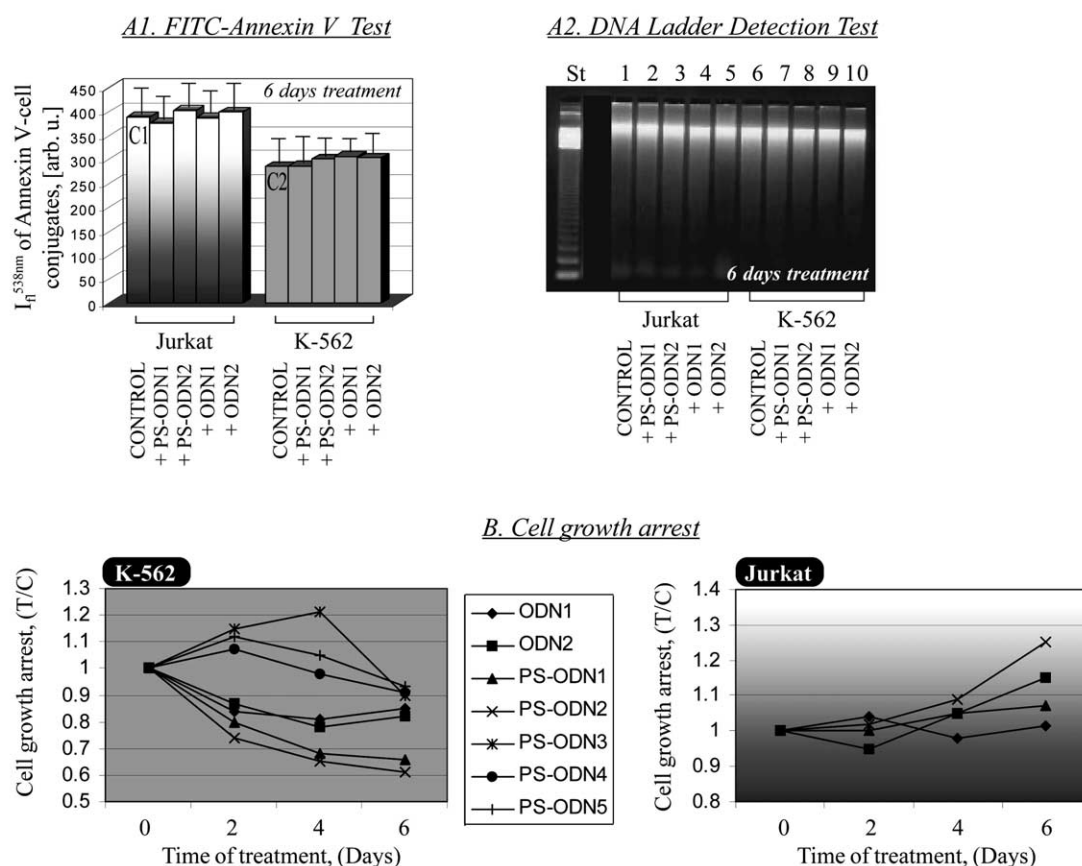
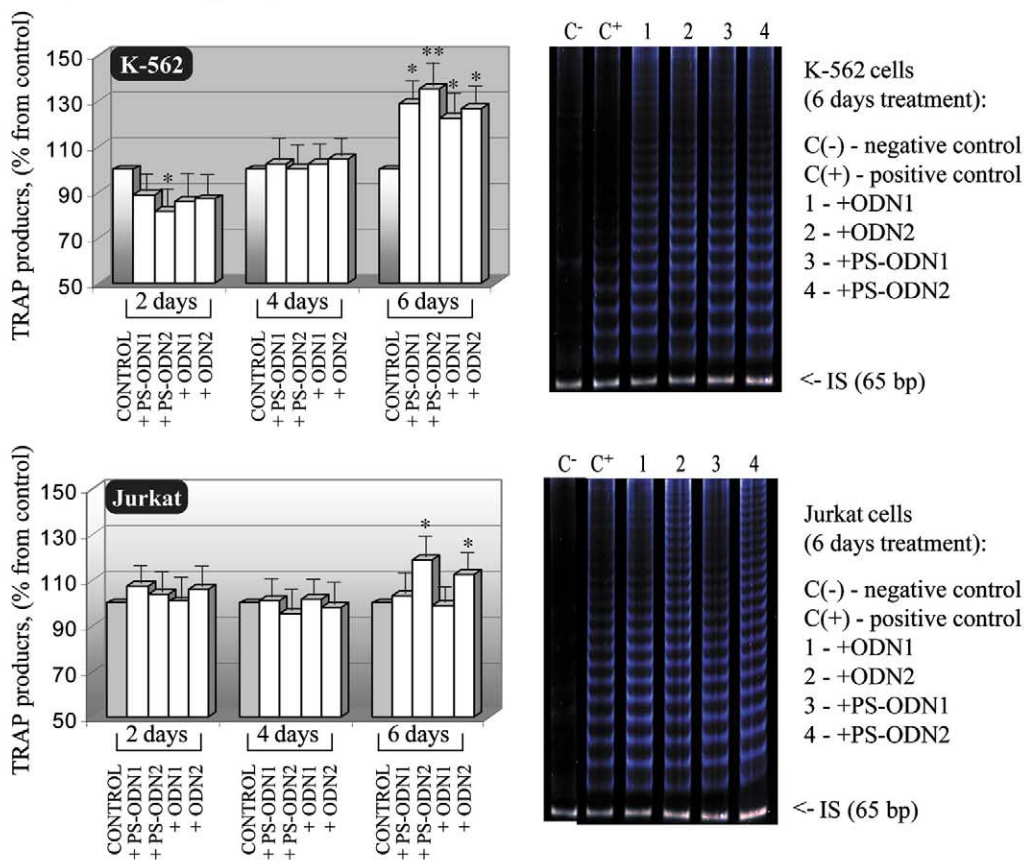


Fig. 3. A: Effect of anti-Bcr-Abl/c-Abl mRNA ODNs (6 days treatment) on the induction of apoptosis in Ph(+) K-562 and Ph(–) Jurkat cells. A1: Annexin V-FITC test for detection of apoptosis (Beckman Coulter). Cells were cultured during 6 days as described in Fig. 1D and collected by centrifugation. They were washed twice with PBS and resuspended in annexin binding buffer (2×10^5 cells/ml). The cell suspension was incubated with FITC-conjugated annexin V as described in Section 2. FITC-annexin V, bound to PSer on the cell surface, was detected spectrofluorometrically at $\lambda_{ex} = 488$ nm and $\lambda_{em} = 535$ nm. The data are presented as means \pm S.D. from six independent experiments. Control groups are representative for non-treated cells, cells treated with lipofectamine only, and for cells transfected with sense or nonsense ODNs/PS-ODNs. A2: DNA ladder detection test (Waco). The test is based on the fact that DNA from apoptotic cells forms a ladder on the gel, while DNA from non-apoptotic cells appears as a single band or smeared on the gel. Cells were cultured during 6 days as described in Fig. 1D and collected by centrifugation. Cell lysis and DNA isolation were carried out according to the test's protocol. DNA was analyzed by TBA electrophoresis in 6% polyacrylamide gel. Gels were stained with SYBR Green. St, standard marker (stable 100 bp DNA ladder, Sigma). Four independent experiments were carried out. Blots from one typical experiment are shown in the figure. Note that no DNA fragmentation was detected in antisense-treated leukemic cells. Control blots are representative for cells treated with lipofectamine only, and for cells transfected with sense or nonsense ODNs/PS-ODNs. B: Effect of anti-Bcr-Abl/c-Abl mRNA ODNs on the amount of viable cells. Cells were cultured in the presence or in the absence of antisense ODNs as described in Fig. 1D. At each time point the amount of viable cells in proliferation was detected spectrophotometrically, based on the reduction of MTS into a formazan product (absorbance at 490 nm). The data were calculated as T/C , where T is OD_{490nm} of ODN-treated cells, and C is OD_{490nm} of non-treated cells. They are presented as mean values from nine independent experiments. S.D. values did not exceed 10% of the respective mean value. In the case of K-562, the control group included cells treated with lipofectamine only and cells treated with sense or nonsense ODNs. In the case of Jurkat, the control group included cells treated with lipofectamine only, and cells treated with sense or nonsense ODNs/PS-ODNs.

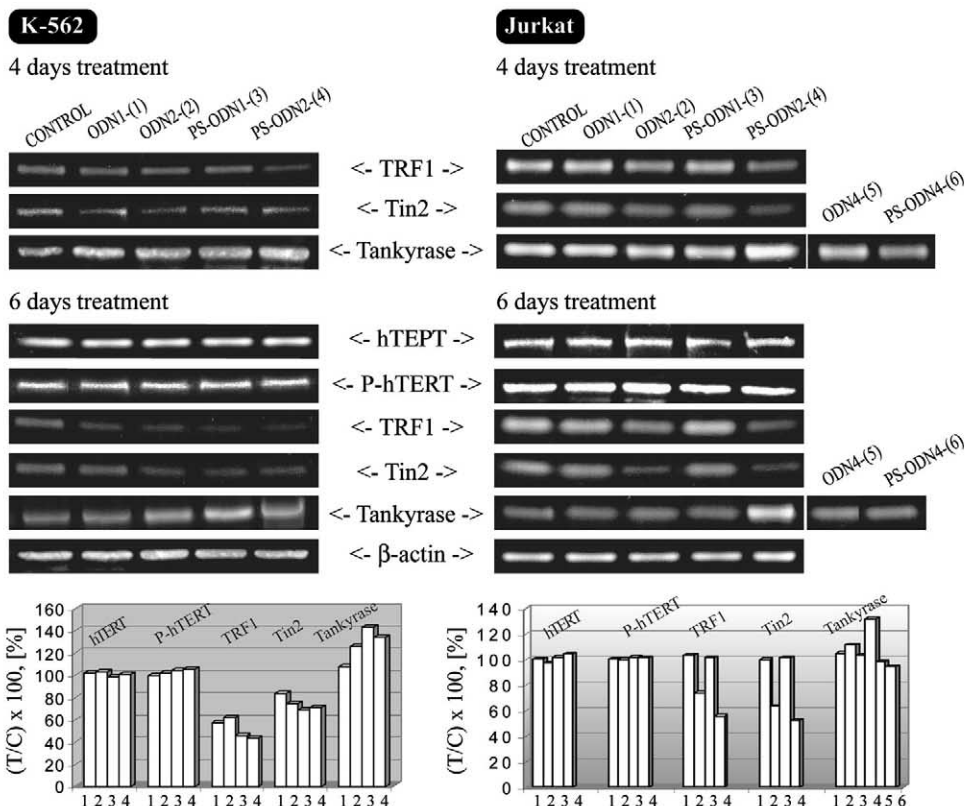
was predominantly into the high density sites of K-562 cells. To guarantee equal experimental conditions and ODN cell concentrations, as well as enough time for re-synthesis of target proteins, transient transfection with lipofectamine was applied for each antisense substance and the cells were treated 'chronically' as shown in Fig. 1D. The selection of the ODN/lipofectamine ratio aimed to avoid the side effects of lipofectamine on cell viability and proliferation. The 'chronic' treatment of cells with antisense substances minimizes their elimination as a result of nuclease degradation [25]. This treatment guarantees most stable steady-state concentrations of the antisense substances in the cells in comparison with single dose application. It allows the expression of effects as a result of a 'long-term' treatment. In preliminary experiments we estab-

lished that 5 μ M ODNs (single dose) decreased the level of p210 Bcr-Abl and the effect was better expressed at 48 h post transfection than after 24 and 72 h. Moreover, the treatment of cells with single dose ODNs did not significantly reduce the level of p210 Bcr-Abl at 72 h post transfection (data not shown). Similar effects have also been reported for Bcr-Abl antisense peptide nucleic acids [23]. Based on these observations, treatment with antisense ODNs every 2 days was applied. Cells treated with lipofectamine only were used as controls. Statistically significant effects of lipofectamine on the parameters analyzed were not detected. Control groups also included the data obtained for cells transfected with nonsense or sense ODNs/PS-ODNs (except in the case of cell growth arrest and tankyrase analyses), because the results were anal-

A. Telomerase activity assay



B. Western blot analysis



ogous to those obtained for non-treated cells and cells treated with lipofectamine only. All control data were pooled together in common control groups.

The capacity of antisense ODNs to reduce the expression of Bcr-Abl and c-Abl in K-562 and Jurkat cells, respectively, was measured by immunoblot analysis and flow cytometry (Fig. 2A,B), using anti-c-Abl antibody with known specificity to 150 kDa c-Abl- and 210 kDa Bcr-Abl-encoded proteins (Sigma). Fig. 2A shows typical Western blots on days 2, 4 and 6 of treatment. The treatment of K-562 cells with PS-ODN1/PS-ODN2 or ODN1/ODN2 markedly reduced the level of p210 Bcr-Abl protein compared to that in non-treated cells even on day 2, and the effect was relatively stable on day 6 (Fig. 2A). Similar results were obtained by flow cytometric registration of the level of Bcr-Abl–antibody complexes, using Fluor-488 IgG-labeled anti-c-Abl antibody (ZenonAlexa) (Fig. 2B). These effects were accompanied by about 60–80% decrease of PTK activity of the immunoprecipitated enzyme and about 45–60% decrease of PTK activity, determined in cell lysates on day 6 (Fig. 2C,D). The effects of PS-ODNs on the level of Bcr-Abl protein and its enzyme activity were better expressed than those of the non-derivatized ODNs. Probably it is a result of the higher stability of PS-ODNs in physiological fluids and cell suspensions in comparison with ODNs [25].

Four days treatment of Jurkat cells with PS-ODN1 or ODN1 did not affect c-Abl protein level, nor its enzyme activity (Fig. 2). This is not surprising since Bcr-Abl fusion protein mRNA does not exist in Jurkat cells and therefore, there is no target for PS-ODN1 and ODN1. These data indicate also that PS derivatization does not provoke non-specific side effects of ODN substances in the concentrations applied. However, the treatment of Jurkat with PS-ODN2 (targeted to Abl mRNA encoding the ATP binding loop) resulted in a decrease of p150 c-Abl protein and the effect was markedly expressed on days 4 and 6 (Fig. 2A,B). It was accompanied by an about 40–60% decrease of PTK activity of Jurkat cells on day 6 (Fig. 2C,D).

The effects of antisense substances on Bcr-Abl/c-Abl were not a result of cytotoxicity and induction of apoptosis. ODNs did not manifest significant cytotoxic effects against K-562 and Jurkat, determined by the cellular ATP bioluminescence

(data not shown). They did not induce apoptosis, estimated by PSer exposure on the cell surface or by DNA fragmentation (Fig. 3A1,A2). However, all substances significantly decreased the cell growth of K-562 and did not provoke cell growth arrest in Jurkat (Fig. 3B). Moreover, the treatment with PS-ODN2 significantly increased the number of viable Jurkat cells on days 4 and 6. PS-derivatized sense and non-sense ODNs manifested poor antiproliferating activity after 6 days treatment of K-562 cells, probably as a result of a non-specific effect of phosphorothioate on this parameter.

To clarify whether the changes in Bcr-Abl/c-Abl origin influence telomerase, the telomerase activity was evaluated at each time point of the cell treatment, using a conventional TRAP and Stretch PCR [14]. Fig. 4A shows that during 2 days treatment the telomerase activity decreased slightly in K-562 cells (~10–15%), this effect disappeared on day 4 and reverted to a significant increase of telomerase activity (~30%) on day 6. Although the viability and proliferating activity of K-562 cells are very sensitive to the amount of Bcr-Abl fusion protein (cell growth arrest was shown in Fig. 3B), it seems that the cells keep a potential to restore proliferation and immortalization through telomerase activation.

The alteration of the telomerase activity of K-562 was not accompanied by variations in its catalytic subunit. The hTERT level was constant during 6 days treatment. No variations were detected either in phospho-Tyr-hTERT (Fig. 3B, 6 days treatment). This puts into doubt the hypothesis that the increased telomerase activity in ODN-treated K-562 cells is a result of decreased Tyr phosphorylation of telomerase by Bcr-Abl. Presumably, in native cells the cross-talk between both enzymes was not mainly mediated through the Tyr phosphorylation/dephosphorylation pathway and the link between both enzymes is indirect.

In the last 3–4 years it has been established that the telomerase-mediated telomere elongation in cancer cells is tightly regulated not only by hTERT status and integrity of the telomerase molecule, but also by several telomeric-associated proteins (TRF1, TRF2, Tin2, tankyrase, Rap1) that regulate the access of telomerase to the telomeres [26–31]. The accent in our work was on TRF1 (telomeric repeat binding factor, a 56 kDa protein) and Tin2 (~40 kDa protein), which have

Fig. 4. A: Telomerase activity assay in Ph(+) K-562 and Ph(–) Jurkat cells, treated with antisense Bcr-Abl/c-Abl mRNA ODNs. Telomerase activity was detected by conventional TRAP and Stretch PCR. Nine independent assays for each sample were performed. The concentration of TRAP products was detected spectrophotometrically at $\lambda=450$ nm, and the results were calculated as a percentage of the subsequent positive control (C1, C2). The mean absorbance of controls at 450 nm for all time points was 1.846 ± 0.205 for Jurkat and 1.057 ± 0.083 for K-562. The absorbance of negative controls at 450 nm was 0.155 ± 0.028 and this value was subtracted from each result. * $P < 0.05$ vs. control group, ** $P < 0.01$ vs. control group, *** $P < 0.001$ vs. control group. Blots from one typical experiment after 6 days treatment are also shown in the figure. Positive controls are representative for cell lysates, obtained from antisense non-treated cells, cells treated with lipofectamine only, and for cells transfected with sense or nonsense ODNs/PS-ODNs. Negative controls are representative for cell lysates (obtained from treated or non-treated cells), subjected to 70°C for 10 min, before initiating of telomerase reaction. B: Levels of hTERT, TRF1, Tin2 and tankyrase in Ph(+) K-562 and Ph(–) Jurkat cells, treated with antisense Bcr-Abl/c-Abl mRNA ODNs – Western blot analysis. Cells were lysed by Telo-Chaser buffer (for hTERT analysis) or by TNE buffer (for TRF1, Tin2 or tankyrase analysis). Cell lysates were suspended 1:1 (v/v) in 2×Laemmli buffer and the samples were fractionated by 5% stacking, 8% resolving (for hTERT) or 4–20% resolving SDS–polyacrylamide gel (for TRF1, Tin2 and tankyrase). Proteins were immunoblotted as described in Section 2. The following primary antibodies were used: anti-hTERT (rabbit, Calbiochem, 0.4 µg/ml), anti-tankyrase (rabbit, Calbiochem, 0.1 µg/ml), anti-TRF1 (rabbit, Calbiochem, 0.7 µg/ml), anti-Tin2 (mouse, Calbiochem, 0.5 µg/ml), anti-β-actin (mouse, Sigma, 0.1 µg/ml). The respective secondary antibodies (goat anti-rabbit or anti-mouse IgG), conjugated with HRP, were applied. Chemiluminescence of the blots was detected immediately using ECL Advance Western Blotting Detection kit. Seven independent experiments for hTERT and six for tankyrase, TRF1 and Tin2 were carried out. Blots from one typical experiment for each protein are shown in the figure. The histograms show T/C , where T is the chemiluminescence of the blots obtained from antisense-treated cells, and C is the chemiluminescence of the blots obtained from control untreated cells. In the case of hTERT, TRF1 and Tin2, control blots are representative for antisense non-treated cells, cells treated with lipofectamine only, and for cells transfected with sense or nonsense ODNs/PS-ODNs. In the case of tankyrase in Jurkat, control blots are representative for antisense non-treated cells, cells treated with lipofectamine only, and for cells transfected with sense ODN3/PS-ODN3 or nonsense ODN5/PS-ODN5.

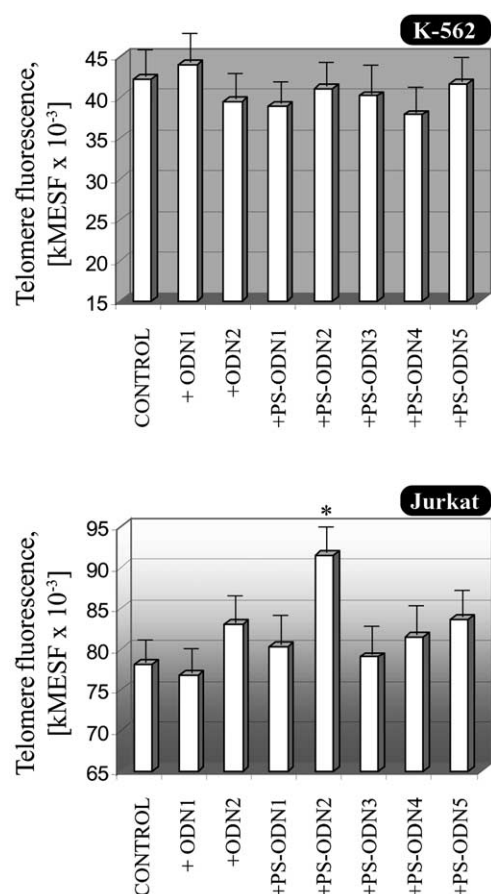


Fig. 5. Flow-FISH telomere fluorescence performed in K-562 and Jurkat cells, treated with antisense Bcr-Abl/c-Abl mRNA ODNs. The flow cytometry-based method using FISH with FITC-labeled PNA probe was applied for detection of telomere length in the cells before and after 6 days treatment with antisense Bcr-Abl/c-Abl mRNA ODNs. Cells hybridized without FITC-labeled telomere PNA probe were used to correct their autofluorescence. The telomere fluorescence of cells was calculated by subtraction of the autofluorescence of unstained controls from the telomere fluorescence measured in cells hybridized with the FITC-labeled telomere PNA probe. The results are expressed as telomere fluorescence in MESF and are the means \pm S.E.M. from five independent experiments. The control group included non-treated cells and cells treated with lipofectamine only. * $P < 0.05$ vs. control group.

been identified as negative regulators of the telomerase function, and on tankyrase (a 142 kDa protein, poly-(ADP-ribose)-polymerase), which has been accepted as a positive regulator [27–30]. The interaction between these three factors seems to be simple and strongly organized to control the access of telomeric TTAGGG repeats to telomerase. Tin2/TRF1 has been found to interact with telomeric DNA and to remodel DNA configuration. This suppresses the access of telomeric repeats for telomerase. Tankyrase has been identified as a TRF1-interacting factor [30]. Tankyrase-mediated poly-(ADP-ribosylation) of TRF1 induces the release of TRF1 from telomeres, opening up the telomeric complex and allowing the access to telomerase [30,31]. All these factors did not directly modulate the telomerase.

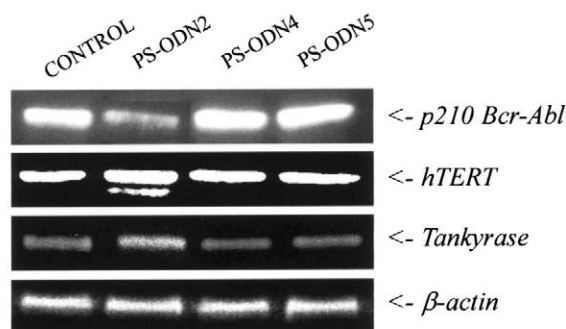
To evaluate whether the decreased amount of Bcr-Abl affects this mechanism of telomere length control, we determined the levels of TRF1, Tin2 and tankyrase in ODN-treated and non-treated cells, using adequate antibodies

(anti-TRF1, anti-Tin2 and anti-tankyrase) and immunoblot analysis. Because the endogenous TRF1 and Tin2 are usually not highly expressed in CML, several modifications of the standard Western blot procedures were made to identify both substances in non-treated and treated K-562 cells [27,28]. The results in Fig. 4B show that the amounts of TRF1 and Tin2 decreased markedly in ODN-treated K-562 cells on days 4 and 6, while the amount of tankyrase increased slightly on day 4, and significantly on day 6. The results suggest that the anti-Bcr-Abl mRNA-treated K-562 cells keep a potential for indirect induction of telomerase activity through overexpression of tankyrase and decreased expression of Tin2/TRF1. These variations in telomeric-associated proteins can provoke most free access of telomeres for the telomerase and positive telomerase control, as well as enhancing the possibility for 'alternative telomere lengthening'. We established also that the growth arrest of K-562 goes to a plateau during 6 days treatment with anti-Bcr-Abl ODNs (Fig. 3B). However, no telomere elongation was observed during 6 days treatment, detected by flow-FISH analysis (Fig. 5). Telomere length was relatively stable during treatment – indirect evidence that the cells keep their proliferation capacity.

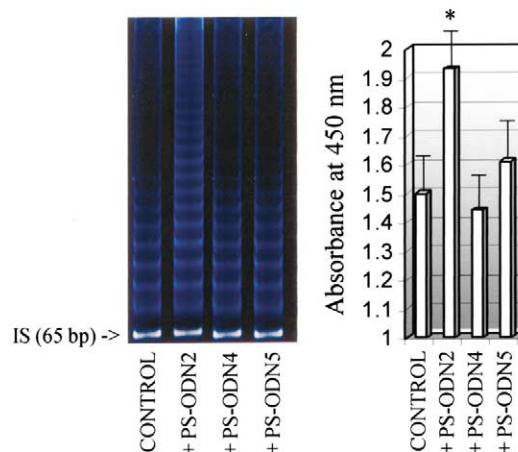
Recently Brummendorf and colleagues have reported an extension of the telomeres in CML patients after long-term treatment with the Bcr-Abl tyrosine kinase inhibitor Glivec [32] in both chronic phase and blast crisis. Analyzing 517 samples from 206 patients the authors established that telomere length from the start of treatment up to day 144 is significantly shorter compared to patients treated for more than 144 days. In patients with repeated measurements, a significant increase in telomere length under treatment is observed. Median telomere length in major remission has been found to be significantly longer in comparison to patients without response to treatment, measured either by cytogenetics, interphase FISH, or quantitative reverse transcription PCR. However, the authors did not investigate the mechanism of telomere elongation and the effect of Glivec on the factors potentially responsible for this process.

Obviously, there is a possibility for telomere elongation after long-term treatment of Ph(+) cells with Bcr-Abl inhibitors. To verify this assumption we used the following experimental protocol: K-562 cells were treated during 36 days with PS-ODN2 on the scheme shown in Fig. 1D. However, to avoid the side effects of lipofectamine during many transfection procedures, we applied PS-ODN2 every 2 days in a single dose of 5 μ M without any transfection. The results in Fig. 6 demonstrate that the long-term treatment of K-562 with PS-ODN2 induced a significant telomere elongation, accompanied by overexpression of tankyrase and increased telomerase activity. Moreover, overexpression of hTERT was also detected, which was not observed during short-term treatment (6 days). This may give rise to speculation that Bcr-Abl is responsible for regulation of hTERT expression and/or its synthesis and the long-term treatment with anti-Bcr-Abl substances makes it possible to detect the relationship between both oncogenes/oncoproteins. Obviously, a cross-talk exists between them and it is necessary to verify whether it is direct or mediated by other factors, which will be our future effort. It seems that the cells treated with anti-Bcr-Abl mRNA substances are adapted to the decreased amount of Bcr-Abl protein and trigger some other compensatory mechanism for preservation of the proliferation as telomerase activation.

A. Western blot analysis of Bcr-Abl, hTERT and Tankyrase
(K-562 - 36 days treatment)



B. Telomerase activity assay
(K-562 - 36 days treatment)



C. Flow-FISH analysis of telomere length
(K-562 - 36 days treatment)

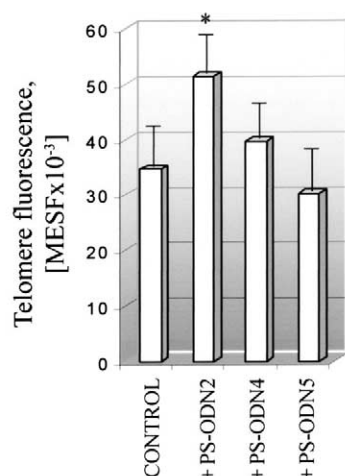


Fig. 6. A: Levels of Bcr-Abl, hTERT, and tankyrase in K-562 after long-term treatment with PS-ODN2 (36 days) – Western blot analysis. Cells were lysed by TeloChaser buffer (for hTERT analysis) or by TNE buffer (for tankyrase analysis). Cell lysates were suspended 1:1 (v/v) in 2×Laemmli buffer and the samples were fractionated by 5% stacking, 8% resolving (for hTERT) or 4–20% resolving SDS–polyacrylamide gel (for tankyrase). Proteins were immunoblotted as described in Section 2. The following primary antibodies were used: anti-hTERT (rabbit, Calbiochem, 0.4 µg/ml), anti-tankyrase (rabbit, Calbiochem, 0.1 µg/ml), anti-β-actin (mouse, Sigma, 0.1 µg/ml). The respective secondary antibodies (goat anti-rabbit or anti-mouse IgG), conjugated with HRP, were applied. Chemiluminescence of the blots was detected immediately using ECL Advance Western Blotting Detection kit. Six independent experiments for each protein were carried out. Blots from one typical experiment for each protein are shown in the figure. Control blots are representative for non-treated cells. B: Telomerase activity assay in K-562 after long-term treatment with PS-ODN2 (36 days). Telomerase activity was detected by conventional TRAP and Stretch PCR. Six independent assays for each sample were performed. The concentration of TRAP products was detected spectrophotometrically at $\lambda = 450$ nm. The absorbance of negative controls at 450 nm was subtracted from each result. * $P < 0.05$ vs. control group. Blots from one typical experiment are also shown in the figure. Controls are representative for cell lysates, obtained from non-treated cells. C: Flow-FISH telomere fluorescence performed in K-562 after long-term treatment with PS-ODN2 (36 days). The flow cytometry-based method using FISH with FITC-labeled PNA probe was applied for detection of telomere length in the cells before and after 36 days treatment with antisense PS-ODN2, sense PS-ODN4 or nonsense PS-ODN5. Cells hybridized without FITC-labeled telomere PNA probe were used to correct their autofluorescence. The telomere fluorescence of cells was calculated by subtraction of the autofluorescence of unstained controls from the telomere fluorescence measured in cells hybridized with the FITC-labeled telomere PNA probe. The results are expressed as telomere fluorescence in MESF and are the means \pm S.E.M. from six independent experiments. Control group included non-treated cells. * $P < 0.05$ vs. control group.

The relationship between Abl tyrosine kinase and telomerase was confirmed also from the results on Jurkat cells. It was established that the telomerase activity increased on day 6 in anti-c-Abl mRNA-treated Jurkat cells (ODN2, PS-ODN2). This effect was accompanied by a decrease in TRF1 and Tin2 on days 4–6, a significant increase of tankyrase even on day 4 (in PS-ODN2-treated cells), enhancement of the number of viable cells in proliferation (Figs. 3B and 4) and

telomere elongation during 6 days treatment with PS-ODN2 (Fig. 5). Converting MESF values into kilobases by the equation described by Baerlocher and Lansdorp [18], it was established that in Jurkat cells the mean telomere length increased from 4.356 kb in control cells to 5.139 kb even after 6 days treatment with PS-ODN2 ($P < 0.05$).

In conclusion, the present study provides evidence that cross-talk exists between Bcr-Abl/c-Abl tyrosine kinase and

telomerase in CML/ALL cells respectively, and the relatively long-term inhibition of the synthesis of Bcr-Abl/c-Abl proteins keeps a potential for restoration of cell proliferation through telomerase activation and/or overexpression of tankyrase. These observations provoke a question: does this mechanism take place in the development of resistance to the highly selective Bcr-Abl drugs, applied in CML therapy? It seems that two independent effects can be accumulated after long-term treatment with anti-Bcr-Abl substances – reactivation of Bcr-Abl amplification as a result of point mutations in the Abl kinase domain [19–21], and/or continued suppression of Bcr-Abl synthesis, accompanied by an induction of alternative telomerase-dependent signaling pathways. Both mechanisms lead to restoration of abnormal proliferation of leukemia cells. In this context, the combined application of anti-Bcr-Abl drugs and substances influencing telomere lengthening may be a promising strategy in CML control. Recently published data, demonstrating that the inhibition of human telomerase enhances the effect of the tyrosine kinase inhibitor Glivec in Ph(+) cells, support this assumption [33].

Acknowledgements: This study was supported in part by the JSPS Invitation Fellowship Program for Research in Japan.

References

- [1] Van Etten, R.A. (2002) *Oncogene* 21, 8643–8651.
- [2] O'Dwyer, M.E., Mauro, M.J. and Druker, B.J. (2002) *Annu. Rev. Med.* 53, 369–381.
- [3] Wisniewski, D., Lambek, C.L., Liu, C., Strife, A., Veach, D.R., Nagar, B., Young, M.A., Schindler, T., Bornmann, W.G., Bertino, J.R., Kuriyan, J. and Clarkson, D. (2002) *Cancer Res.* 62, 4244–4255.
- [4] Fabbro, D., Ruetz, S., Buchdunger, E., Cowan-Jacob, S.W., Fendrich, G., Liebetanz, J., Mestan, J., O'Reilly, T., Traxler, P., Chaudhuri, B., Fretz, H., Zimmermann, J., Meyer, T., Caravatti, G., Furet, P. and Manley, P.W. (2002) *Pharmacol. Ther.* 93, 78–98.
- [5] Ohyashiki, K., Ohyashiki, J.H., Iwata, H., Hayashi, S., Shay, J.W. and Toyama, K. (1997) *Leukemia* 11, 190–194.
- [6] Engelhardt, M., Mackenzie, K., Drullinsky, P., Silver, R.T. and Moore, M.A. (2000) *Cancer Res.* 60, 610–617.
- [7] Ohyashiki, K., Sashida, G., Tauchi, T. and Ohyashiki, K. (2002) *Oncogene* 21, 680–687.
- [8] Feng, J., Funk, W.D., Wang, S.S., Weinrich, S.L., Avilion, A.A., Chiu, C.P., Adams, R.R., Chang, E., Allsoop, R.C. and Yu, J. et al. (1995) *Science* 269, 1236–1241.
- [9] Weinrich, S.L., Pruzan, R., Ma, L., Ouellette, M., Tesmer, V.A., Holt, S.E., Bodnar, A.G., Lichtsteiner, S., Kim, N.W., Trager, J.B., Taylor, R.D., Carlos, R., Andrews, W.H., Wright, W.E., Shay, J.W., Harley, C.B. and Morin, G.B. (1997) *Nat. Genet.* 17, 498–502.
- [10] Kyo, S. and Inoue, M. (2002) *Oncogene* 21, 688–697.
- [11] Yu, C.C., Lo, S.C. and Wang, T.C. (2001) *Biochem. J.* 355, 459–464.
- [12] Kharbanda, S., Kumar, V., Dhar, S., Pandey, P., Chen, C., Majumder, P., Yuan, Z.M., Strauss, W., Pandita, T.K., Weaver, D. and Kufe, D. (2000) *Curr. Biol.* 10, 568–575.
- [13] Jamieson, L., Carpenter, L., Biden, T.J. and Fields, A.P. (1999) *J. Biol. Chem.* 274, 3927–3930.
- [14] Tatematsu, K., Nakayama, J., Danbara, M., Shiomoya, S., Sato, H., Omine, M. and Ishikawa, E. (1996) *Oncogene* 13, 2265–2274.
- [15] Li, H., Zhao, L., Yang, Z., Funder, J.W. and Liu, J.P. (2002) *J. Biol. Chem.* 273, 33436–33442.
- [16] Mosmann, T. (1983) *J. Immunol. Methods* 65, 55–63.
- [17] Baerlocher, G.M., Mak, J., Tien, T. and Lansdorp, P.M. (2002) *Cytometry* 47, 89–99.
- [18] Baerlocher, G.M. and Lansdorp, P.M. (2003) *Cytometry* 55A, 1–6.
- [19] Gorre, M.E., Mohammed, M., Ellwood, K., Hsu, N., Paquette, R., Rao, P.N. and Sawyers, C.L. (2001) *Science* 293, 876–880.
- [20] Von Bubnoff, N., Schneller, F., Peschel, S. and Duyster, J. (2002) *Lancet* 359, 487–491.
- [21] Hofmann, W.K., Jones, L.C., Lemp, N.A., de Vos, S., Gschaidmeier, H., Hoelzer, D., Ottmann, O.G. and Koeffler, H.P. (2002) *Blood* 99, 1860–1862.
- [22] Buchardt, O., Egholm, M., Berg, R.H. and Nilsen, P.E. (1993) *Trends Biochem.* 11, 384–386.
- [23] Rapozzi, V., Burm, B.E.A., Cogoi, S. and Van der Marel, G.A. (2002) *Nucleic Acids Res.* 30, 3712–3721.
- [24] Norton, J., Piatyszek, M.A., Wright, W.E., Shay, J.W. and Corey, D.R. (1996) *Nat. Biotechnol.* 14, 615–619.
- [25] Kurreck, J. (2003) *Eur. J. Biochem.* 270, 1628–1644.
- [26] Bianchi, A., Smith, S., Chong, L., Elias, P. and De Lange, T. (1997) *EMBO J.* 16, 1785–1794.
- [27] Ohyashiki, J.H., Hayashi, S., Yahata, N., Iwama, H., Ando, K., Tauchi, T. and Ohyashiki, K. (2001) *Int. J. Oncol.* 18, 593–598.
- [28] Cook, B.D., Dynek, J.N., Chang, W., Shostak, G. and Smith, S. (2002) *Mol. Cell. Biol.* 22, 332–342.
- [29] Loayza, D. and De Lange, T. (2003) *Nature* 423, 1013–1018.
- [30] Smith, S. and De Lange, T. (2000) *Curr. Biol.* 10, 1299–1302.
- [31] Smith, S., Gariat, I., Schmitt, A. and De Lange, T. (1998) *Science* 282, 1484–1487.
- [32] Brummendorf, T.H., Ersoz, I., Hartmann, U., Balabanov, S., Wolke, H., Paschka, P., Lahaye, T., Berner, B., Bartolovic, K., Kreil, S., Berger, U., Gschaidmeier, H., Bokemeyer, C., Hehlmann, R., Dietz, K., Lansdorp, P.M., Kanz, L. and Hochhaus, A. (2003) *Ann. NY Acad. Sci.* 996, 26–38.
- [33] Tauchi, Y., Nakajima, A., Sashida, G., Shimamoto, T., Ohyashiki, J.H., Abe, K., Yamamoto, K. and Ohyashiki, K. (2002) *Clin. Cancer Res.* 8, 3341–3347.